$\mathcal{PT}-$Symmetry and Supersymmetry: Interconnection of Broken and Unbroken Phases

Adipta Pal*[1], Subhrajit Modak [†2], Aradhya Shukla [‡3], and Prasanta K. Panigrahi[§3]

[1]Max Planck Institute for the Physics of Complex Systems,

Nöthnitzer Straße 38, D-01187 Dresden, Germany

[2] Indian Institute of Science Education and Research Mohali,

Punjab - 140306, India

[3]Indian Institute of Science Education and Research Kolkata, Mohanpur,

West Bengal - 741246, India

Abstract

The broken and unbroken phases of $\mathcal{PT}$ and supersymmetry in optical systems are explored for a complex refractive index profile in the form of a Scarf potential, under the framework of supersymmetric quantum mechanics. The transition from unbroken to the broken phases of $\mathcal{PT}-$symmetry, with the merger of eigenfunctions near the exceptional point is found to arise from two distinct realizations of the potential, originating from the underlying supersymmetry. Interestingly, in $\mathcal{PT}$-symmetric phase, spontaneous breaking of supersymmetry occurs in a parametric domain, possessing non-trivial shape invariances, under reparametrization to yield the corresponding energy spectra. One also observes a parametric bifurcation behaviour in this domain. Unlike the real Scarf potential, in $\mathcal{PT}-$symmetric phase, a connection between complex isospectral super-potentials and modified KdV equation occurs, only with certain restrictive parametric conditions. In the broken $\mathcal{PT}$-symmetry phase, supersymmetry is found to be intact in the entire parameter domain yielding the complex energy spectra, with zero-width resonance occurring at integral values of a potential parameter.

1 Introduction

The search for new materials with desired optical properties has been one of the main driving forces of research in optics and other related areas in recent times [1, 2, 3]. Emergence of

---

*adiptapal7@gmail.com

†modoksuvrojit@gmail.com

‡aradhya02@iiserkol.ac.in

§pprasanta@iiserkol.ac.in

Parity-Time ($\mathcal{PT}$)-symmetric [4, 5] optical structures represent a new generation of artificial optical systems [6, 7], which utilize gain and loss in a balanced manner to achieve desired order of functionality [8, 9]. Among these developments, $\mathcal{PT}-$symmetric laser [10], the realization of anti $\mathcal{PT}$-symmetry in microcavity [11, 12] and the ultrasensitive electromagnetic sensors [13] are worth mentioning. The careful balancing of loss and gain is now being overcome through gain-free route by using appropriate designed passive systems [14, 15]. Recent observation of unbroken and broken phases of $\mathcal{PT}-$symmetry in photonic condensates near equilibrium condition, has opened further avenues for both physical and technological applications [16]. Interestingly, supersymmetry, a proposed symmetry interconnecting fundamental bosons and fermions [17], has been successfully used for controlled lasing [18, 19, 20] and other optical applications [21]. Supersymmetry has been found very useful in phase-matched mode selection, removal of undesired modes and other phase-sensitive applications [22]. It plays a crucial role in designing $\mathcal{PT}$ inspired optical couplers [23, 24]. Both these symmetries are characterized by unbroken and broken phases, having different physical properties in optical systems. Balancing of gain and loss plays the key role in realizing the broken and unbroken phases of $\mathcal{PT}-$symmetry, dramatically changing behaviour of light propagation in the medium [25, 26]. At the symmetry breaking point, light can be brought to a complete stop [27]. Supersymmetry in optical and quantum mechanical systems, interconnects even and odd eigenfunctions of two distinct systems [28, 29]. Interestingly, an additional symmetry, known as shape invariance (SI) characterizes certain systems, where the potential or the refractive index profiles of the supersymmetric partners have same functional form, differing only in their constant parameters [30, 31]. The energy values are analytically calculable in this case, allowing one to tune the potential parameters to achieve a desired level [32]. The potentials can be further tuned using the iso-spectral deformation, which enables one to modify the wavefuntion and the potential profile, keeping the eigenvelues intact. This has found use in explaining the resonance width in physical systems [33] and tailoring of the optical fibers for desired beam profile [34, 35, 36]. Expectedly, a system with both $\mathcal{PT}$ and supersymmetry can provide significant control of medium properties. As the broken and unbroken phases of these two symmetries depend on the potential parameters, a careful identification of the parameter domain for the two physically distinct phases is worth investigating. $\mathcal{PT}-$symmetry came into play after the seminal work of Bender and Boettcher [4, 5], in which they suggested an extension of quantum mechanics, where the notion of Hermiticity of the underlying Hamiltonian is replaced by $\mathcal{PT}$ invariance. As an example, a $\mathcal{PT}-$symmetric Hamiltonian contains a one-dimensional Schrödinger operator with a complex potential satisfying $V(x) = V^*(-x)$, i.e., the real and imaginary parts of the potential must be symmetric and anti-symmetric functions, respectively. Such non-Hermitian systems exhibit many interesting properties, which are otherwise unattainable in conventional Hermitian systems. One of the most striking $\mathcal{PT}$ properties is the appearance of a sharp, symmetry-breaking transition [37], once the non-Hermitian parameter crosses a certain threshold. This transition signifies the occurrence of a spontaneous $\mathcal{PT}-$symmetry breaking from the exact phase, where all of the eigenvalues are real, to a broken phase where eigenvalues occur in complex-conjugate pairs. This symmetry breaking point is termed as exceptional point, where the eigenvalues coalesce and the corresponding eigenvectors collapse on each other. Exceptional points have been observed in

various photonic systems [38], optical waveguides [21] and time domain lattices [39].

In optical systems, Helmholtz equation replaces the Schrödinger equation, enabling the well-established quantum mechanical tools for use in optical systems. In order to realize complex $\mathcal{PT}-$symmetric structures, this formal equivalence of the quantum mechanical Schrödinger equation to the optical wave equation has been exploited by combining symmetric index guiding with an antisymmetric gain/loss profile [40, 41]. The prospect of utilizing both optical gain and loss has emerged as a new paradigm in shaping the flow of light. These include effects like unidirectional invisibility [42], loss-induced transparency [7], band merging [43], optically induced atomic lattices [44] and improved lasing as mentioned earlier. The exceptional points (EPs) have emerged as a new design tool for engineering the response of optical systems, as near these points, light propagation has a strong parameter sensitivity, which is further affected by subtle changes in the initial condition [45]. Such behaviour is characteristic of classical and quantum catastrophes [46]. Recent studies have shown that controllable confinement of light can be made possible at EPs [47]. The physical phenomena near EPs reveal many interesting features, like negative refractive index [48] and Bloch oscillation in complex crystals [49, 50]. For an account of the recent status of $\mathcal{PT}$-symmetry, the interested readers are referred to [51].

Here, we investigate the Helmholtz equation for light propagation through a medium, having complexified dielectric distribution, obeying $\mathcal{PT}-$symmetry. For explicitness, we consider complex Scarf profile as refractive index, where all the aforementioned features of $\mathcal{PT}-$symmetric system are analytically tractable. The refractive index profile, in the form of a Scarf potential in the Helmholtz equation, has been recently designed for controlling reflection of light, which at certain parameter value can be completely reflectionless [52, 53]. Interestingly, the complex Scarf potential is also characterized by supersymmetry (SUSY), which provides a new avenue for designing partner index profiles with desired characters [54]. It can serve as a testing platform, where ramifications of SUSY and $\mathcal{PT}$-symmetry can be explored and utilized to realize new class of functional structures.

The paper is organized as follows. Section 2 establishes the connection between the refractive index profile of the Helmholtz equation and $\mathcal{PT}-$symmetric potential in quantum mechanics, together with a brief discussion about fundamentals of supersymmetric quantum mechanics (SUSY QM). In section 3, the complex $\mathcal{PT}-$symmetric potential is introduced and analysed in terms of SUSY methods, while establishing their connection with optics. The phases of $\mathcal{PT}-$symmetry and SUSY and their interconnection have been discussed in section 4. The spectral structures and parameter domain for SUSY broken phases are derived for the first time for the complex Scarf II potential. Subsection 4.1 makes a connection between the spectral problem in unbroken phase and modified KdV equation through isospectral deformation. The subsequent subsection shows another feature of the $\mathcal{PT}-$phase transition, bifurcation phenomenon in the parameter space, which enables transition from one superpotential to another, interconnecting $\mathcal{PT}-$symmetry with SUSY. Section 5 deals with $\mathcal{PT}-$broken phase, having complex eigenvalues and zero-width resonances, with SUSY intact in the entire parameter domain. Section 6 concludes the paper with directions for future work.

2 Refractive index profile and supersymmetric quantum mechanics

We consider the case of plane monochromatic optical wave incident at an angle θ, in a medium with inhomogeneous dielectric distribution, $\epsilon(x) = \epsilon_b + \alpha(x)$. The inhomogenity is assumed to vanish at spatial infinity, so that $\epsilon(x) \to \epsilon_b$ as $|x| \to \infty$. The problem can be made effectively one dimensional due to the fact that dependence on y is given by $e^{ik_y y}$, where $k_y = k_0 \sqrt{\epsilon_b} \sin\theta$. Note that k_y is same for each layer due to continuity of tangential fields, leading to propagation along the x direction. The propagation equation for transverse electric waves is the Helmholtz equation,

$$\frac{d^2 \mathcal{E}}{dx^2} + (k_0^2 \epsilon(x) - k_y^2)\mathcal{E} = 0, \tag{1}$$

that can be connected with the Schrödinger equation:

$$E = k_0^2 \epsilon_b \cos^2\theta, \tag{2}$$

and

$$V(x) = k_0^2 \epsilon_b - k_0^2 \epsilon(x). \tag{3}$$

The potential $V(x)$ is said to be reflectionless, if it is transparent to waveforms of arbitrary positive energy. The refractive index, $n(x)$, which is the square root of the dielectric function, is related to quantum mechanical potential $V(x)$ (with $\hbar = 2m = 1$):

$$n^2(x) = n_b^2 - \frac{V(x)}{k_0^2}. \tag{4}$$

$\mathcal{PT}$-symmetry requires the refractive index to obey $n(x) = n^*(-x)$. The $\mathcal{PT}-$symmetric potentials with the above optical connection have been at the forefront of investigations [55].

SUSY QM have played a crucial role in revealing interesting facets of various optical systems [56]. SUSY relates two sibling Hamiltonians, which factorize as $H_- = A^\dagger A$ and $H_+ = AA^\dagger$, with $H_\pm = -\frac{\partial^2}{\partial x^2} + V_\pm(x)$. A connection can be established with the introduction of the superpotential, $W(x) = -\frac{1}{\psi_0(x)} \frac{\partial \psi_0(x)}{\partial x}$ for the given pair of potentials:

$$V_\pm = W^2(x) \pm \frac{\partial W(x)}{\partial x}. \tag{5}$$

Here, $\psi_0(x)$ is the ground state of $H_-(x)$, with the ladder operators given by $A^\dagger = -\frac{\partial}{\partial x} + W(x)$, $A = \frac{\partial}{\partial x} + W(x)$. One notices that $E_n^+ = E_{n+1}^-$ and thus, the spectra of partner potentials differ only in the ground state of $H_-(x)$. The eigenvalues and wavefunctions can be explicitly obtained for the shape invariant potentials [32]. Partner potentials are said to be shape invariant, if they satisfy relations of the form,

$$V_+(x; p_0) = V_-(x; p_1) + R(p_1), \tag{6}$$

4

where p_0 is a constant parameter for a given SUSY potential pair, p_1 is a function of p_0 and $R(p_1)$ is a constant function independent of x. The spectrum of $H_-(x)$ is obtained as

$$E_0^n = \sum_{k=1}^{n} R(p_k), \tag{7}$$

and the eigenstates are explicitly given by,

$$\psi_n^-(x; p_0) \propto A^\dagger(x; p_0) A^\dagger(x; p_1)...A^\dagger(x; p_{n-1})\psi_0^-(x, p_n). \tag{8}$$

The SUSY method can be used to determine the energy spectra in a number of $\mathcal{PT}-$symmetric complex potential [37], and therefore consequences of $\mathcal{PT}$-symmetry and its breaking can be analytically probed. Some of the potentials also exhibit broken SUSY and hence provide an ideal venue for investigating the broken and unbroken phases of both the symmetries and their interconnection. In the following, for explicitness, we consider the refractive index profile in the form of a Scarf potential, which has found applications for its reflectionless behaviour. In the process, energy spectra in the broken SUSY domain for the complex potential is analytically obtained, through a combination of shape inavriance and SUSY.

3   Broken and unbroken $\mathcal{PT}-$symmetric phases

The real Scarf II potential is one of the exactly solvable potentials, having both bound and scattering states [57]:

$$V(x) = (-A(A + \alpha) + B^2)sech^2\,\alpha x + B(2A + \alpha)sech\,\alpha x\,tanh\,\alpha x, \tag{9}$$

where A, B are real constant parameters. It exhibits many interesting features and has been studied extensively in SUSY quantum mechanics [58], group theory [59, 60] and other approaches [61]. It is a non-symmetric extension of the well studied Pöschl-Teller potential [62]: $V(x) = -A^2\,sech^2 x$, which has been elegantly related to the angular momentum eigenvalue equation [63]:

$$\left[-\frac{1}{sin\theta}\frac{\partial}{\partial\theta}\left(sin\theta\frac{\partial}{\partial\theta} + \frac{m^2}{sin^2\theta}\right)\right] u_l^m(\theta) = l(l + 1)\,u_l^m(\theta), \tag{10}$$

with the mapping $cos\theta = tanh x$:

$$\left[\frac{\partial^2}{\partial x^2} + \frac{l(l + 1)}{sech^2 x}\right] u_l^m(x) = m^2\,u_l^m(x). \tag{11}$$

There are two symmetry operations, $m \to -m$ and $l \to -(l + 1)$, that leave the potential and eigenvalue invariant, which has non-trivial consequences in our analysis. SUSY and shape invariance, combined with the above mentioned parametric freedom find elegant use in obtaining the eigenvalue spectra in both broken and unbroken phases of SUSY [64]. The Scarf II potential can be obtained from superpotential $W(x) = A\,tanh\,\alpha x + B\,sech\,\alpha x$. The

complex $\mathcal{PT}-$symmetric potential can be obtained through a simple parametrization $B \to iB$ [65]:

$$V(x) = (-A(A+\alpha) - B^2)\, sech^2\alpha x + i\, B(2A+\alpha)\, sech\,\alpha x\, tanh\,\alpha x. \qquad (12)$$

for which the eigenspectra and eigenfunctions have been obtained [66]. With the goal of investigating the broken and unbroken phases of $\mathcal{PT}$ and SUSY, we parametrize the generalised complex superpotentials as [37],

$$W_{\mathcal{PT}}^{\pm} = \left(A \pm iC^{\mathcal{PT}}\right) tanh\,\alpha x + \left(\pm\, C^{\mathcal{PT}} + iB\right) sech\,\alpha x, \qquad (13)$$

where all the potential parameters are real. The supersymmetric potential (V_-) corresponding to $W_{\mathcal{PT}}^{\pm}$ is of the form,

$$\begin{aligned}
V_-(x) = (A \pm iC^{\mathcal{PT}})^2 &- \left[(A \pm iC^{\mathcal{PT}})(A \pm iC^{\mathcal{PT}} + \alpha) - (\pm C^{\mathcal{PT}} + iB)^2\right] sech^2\,\alpha x \\
&- i\left(\pm iC^{\mathcal{PT}} - B\right)\left[2(A \pm iC^{\mathcal{PT}}) + \alpha\right] sech\,\alpha x\, tanh\,\alpha x,
\end{aligned} \qquad (14)$$

which leads to both real and complex spectra, physically obtainable using SUSY and shape invariance. The potential in Eq. (14) in general may not be $\mathcal{PT}-$symmetric, for which the coefficient of the first and second terms must be real and purely imaginary, respectively. In the present parametrization, these two conditions lead to a unique relation [37]:

$$C^{\mathcal{PT}}\left[2(A - B) + \alpha\right] = 0. \qquad (15)$$

For $C^{\mathcal{PT}} = 0, \mathcal{PT}-$symmetry is unbroken and one gets bound states with real spectra. However, SUSY is broken in some parametric domains. Nonzero value of $C^{\mathcal{PT}}$ leads to the spontaneous $\mathcal{PT}$ broken phase, where the energy eigenvalues are in general complex. Therefore, $C^{\mathcal{PT}}$ behaves like an order parameter, whose non-vanishing value characterizes broken $\mathcal{PT}$ phase. Interestingly, in both unbroken and broken phases of $\mathcal{PT}$, the potential $V_-(x)$ can be obtained from two distinct superpotentials, due to its underlying symmetry. Interestingly, these two superpotentials generate two disjoint sectors of the Hilbert space in the unbroken case. Here the spectrum is real and shape invariance leads to translational shift in a suitable parameter by real units [37]. For a different parametrization, two different superpotentials lead to the same potential for the broken $\mathcal{PT}-$symmetry as well. In this case, shape invariance produces complex parametric shifts. We discuss in great detail about the interconnection between unbroken $\mathcal{PT}-$symmetric and broken SUSY as well as spontaneously broken $\mathcal{PT}$ phases in the following sections.

4 Unbroken $\mathcal{PT}$ and broken SUSY phases

For $C^{\mathcal{PT}} = 0$, the potential becomes $\mathcal{PT}-$symmetric,

$$V_{\mathcal{PT}}(x) = A^2 - \left[A(A+\alpha) + B^2\right] sech^2\,\alpha x + iB(2A+\alpha) sech\,\alpha x\, tanh\,\alpha x, \qquad (16)$$

derived from the superpotential,

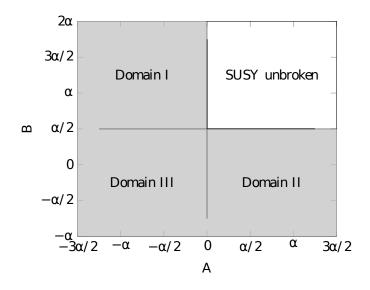$$W_1(x) = A\, tanh\,\alpha x + iB\, sech\,\alpha x. \qquad (17)$$

Figure 1: The shaded regions I, II and III constitute the broken SUSY areas in the parameter space. The energy eigenvalues for the broken SUSY domains can be obtained by considering two shape invariances of the complex $\mathcal{PT}-$symmetric Scarf II potential.

This potential is invariant under the transformation $A \leftrightarrow B - \frac{\alpha}{2}$ [37, 67, 68], which provides another candidate for the superpotential,

$$W_2(x) = (B - \frac{\alpha}{2}) \tanh \alpha x + i(A + \frac{\alpha}{2}) \operatorname{sech} \alpha x. \tag{18}$$

The above mentioned parametric freedom enables two sets of $SL(2,\mathcal{C})$ algebra, which can be mapped onto each other, yielding a unique $\mathcal{PT}-$symmetric potential [69]. These two superpotentials lead to two sets of real energy eigenvalues,

$$E_n^1 = -(A - n\alpha)^2, \tag{19}$$

and

$$E_n^2 = -(B - \frac{\alpha}{2} - n\alpha)^2. \tag{20}$$

valid if, $A > 0$ and $B > \frac{\alpha}{2}$, respectively. For other regions in the parameter space, at least one of the energy eigenvalue set fails to give a normalizable ground state, which points to the case of broken supersymmetry. Interestingly, for the broken SUSY cases, exact energy eigenvalues can be obtained by two steps of shape invariance [70, 71]. One first converts the potential to the SUSY unbroken state and then finds the energy eigenvalues. The regions of broken and unbroken SUSY have been depicted in Fig. 1 . The energy eigenvalues in these regions are obtained as follows:

- **Domain I** ($A < 0$, $B > \alpha/2$): Consider first the shape invariance $A \to -A$ and then apply the known shape invariance $A \to A + \alpha$, to get energy eigenvalues for Eq. (12) as

$$E_{n,I}^1 = -(A + n\alpha)^2, \tag{21}$$

7

E_n^2 remains the same. Notice that the first shape invariance changes the sign of A so that unbroken SUSY can be applied.

- **Domain II** ($A > 0$, $B < \alpha/2$)): Consider first the shape invariance $B - \alpha/2 \rightarrow -(B - \alpha/2)$, $A + \alpha/2 \rightarrow -(A - \alpha/2)$ and then apply the known shape invariance $B - \alpha/2 \rightarrow B - \alpha/2 + \alpha$, $A - \alpha/2 \rightarrow A - \alpha/2$, to get energy eigenvalues as,

$$E_{n,II}^2 = -(B - \frac{\alpha}{2} + n\alpha)^2. \tag{22}$$

E_n^1 remains unchanged. The first shape invariance changes the sign and takes it to the unbroken SUSY domain, sign change for the second parameter does not affect as it does not contribute to the energy for Eq. (18).

- **Domain III** ($A < 0$, $B < \alpha/2$): Here one needs to consider both the techniques, one for Domain I for the eigenvalues of Eq. (17) and one for Domain II for the eigenvalues of Eq. (18), which yields

$$E_{n,III}^1 = -(A + n\alpha)^2, \qquad E_{n,III}^2 = -(B - \frac{\alpha}{2} + n\alpha)^2, \tag{23}$$

in this parametric domain, both the energy spectra change.

It is worth mentioning that the spectral changes can be viewed as the transformation $n \rightarrow -n$. This is identical to the earlier mentioned symmetry $m \rightarrow -m$, in the Pöschl-Teller potential. Analogously, $A \rightarrow -A + \alpha$ is akin to the symmetry $l \rightarrow -(l+1)$. In the following, we illustrate the relationship between superpotenial and modified KdV equation. In subsequent subsection, we discuss about identifying the correct ground state emerging from above two superpotentails and various regions of $\mathcal{PT}$ phases.

4.1 Isospectral deformation and connection with modified KdV equation

The two different superpotentials, giving rise to the same potential, characterise iso-spectral deformation in supersymmetric quantum mechanics. In this, a given potential remains unchanged by an additive deformation of the superpotential, whereas its partner potential is changed having the same energy levels. It is to be noted that superpotential is dependent on the ground state that encodes the boundary conditions, which the potential by itself does not [72]. Thus isospectral deformation only keeps the value of potential ($V_{\mathcal{PT}}$) unchanged, not the system boundaries. It is well-known that, iso-spectral deformation of the superpotentials $\tilde{W}(x) = W(x) + \phi(x)$, leads to the Bernoulli equation:

$$\frac{d\phi(x)}{dx} - 2W_2(x)\phi(x) - \phi^2(x) = 0. \tag{24}$$

For the real Scarf II, $\phi(x)$ satisfies the modified KdV equation [73, 74]. In the case of complex superpotential potential, $W_1(x) = W_2(x) + \phi(x)$, where

$$\begin{aligned}\phi(x) &= (A - B + \alpha/2)\ tanh\,\alpha x + i\ (B - A - \alpha/2)\ sech\,\alpha x \\ &\equiv C\ tanh\,\alpha x + i\ D\ sech\,\alpha x,\end{aligned} \tag{25}$$

the modified KdV equation is satisfied,

$$\frac{\partial \phi}{\partial t} - \phi^2\,\frac{\partial \phi}{\partial x} + \frac{\partial^3 \phi}{\partial x^3} = 0, \tag{26}$$

provided conditions $C = \pm D$. It is evident that condition $C = -D$ is identically satisfied in the case of this present complex superpotential.

4.2   Parameter sensitivity and bifurcation phenomena

We now consider the energy eigenvalues in Eqs. (19) and (20) defined for the two superpotentials in Eq. (17) and Eq. (18) respectively. The lowest energy in both the cases are $-A^2$ and $-(B - \frac{\alpha}{2})^2$ respectively. Therefore, depending on the parameters A and B, we can ascribe the ground state either to $-A^2$ or $-(B - \frac{\alpha}{2})^2$, based on which is lower in energy. Evidently, the superpotential is dependent on the ground state wavefunction, which are different for the two cases and there can be only one ground state in the one dimensional case. Therefore, only the superpotential, corresponding to the lower energy among the mentioned lowest energies, should exist at a given time. The condition for which ground state is allowed with $E_0 = -A^2$, can be expressed as

$$A^2 - (B - \alpha/2)^2 = K^2, \quad K = constant;$$
$$\text{or,} \tag{27}$$
$$\frac{A^2}{K^2} - \frac{(B - \alpha/2)^2}{K^2} = 1,$$

which is a hyperbola in the parameter space of A and B, with the superpotential given in Eq. (17). The contrary condition expressed as:

$$(B - \alpha/2)^2 - A^2 = K_1^2, \quad K_1 = constant;$$
$$\text{or,} \tag{28}$$
$$\frac{(B - \alpha/2)^2}{K_1^2} - \frac{A^2}{K_1^2} = 1$$

yields a conjugate hyperbola to the previous one, such that $-(B - \frac{\alpha}{2})^2$ is the ground state and the superpotential in Eq. (18) holds. Fig. 2 depicts the allowed parameter domains, corresponding to the EP and the zero-width resonance. The allowed regions are bounded by two hyperbolae, where the asymptotes $B = \pm A + \alpha/2$ point to conditions pertaining to the exceptional point and isospectral deformation respectively. The different features of the above figure can be explicated as:
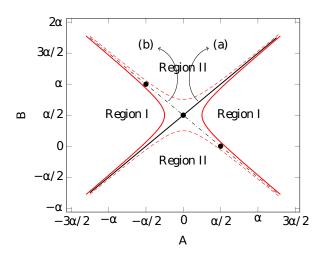
9

Figure 2: Regions I and II correspond to the specific ground states based on the parameters involved. The asymptote with positive slope (a) corresponds to the condition for exceptional point and zero-width resonance while that with negative slope (b) corresponds to isospectral deformation. A small perturbation from the condition for exceptional point or isospectral deformation may lead us to a domain different from the domain of our original trajectory.

- **Region I** contains all the hyperbolae with $-A^2$ as the ground state with superpotential in Eq. (17).

- **Region II** contains all the hyperbolae with $-(B - \frac{\alpha}{2})^2$ as the ground state with superpotential in Eq. (18).

- (a) corresponds to the asymptote given by condition $A = B - \alpha/2$ point and the regime of zero-width resonance.

- (b) is the other asymptote but it is given by the condition $A = -B + \alpha/2$ and is a possible region for real energy eigenvalues and it relates the superpotentials in Eq. (17) and Eq. (18) as **isospectrally deformed** counterparts.

- The coordinate points $(\alpha/2, 0)$ and $(-\alpha/2, \alpha)$ are the only two points lying on asymptote $A = -B + \alpha/2$, on which the isospectral deformation satisfy the **modified KdV equation.**

In region I and region II, each point on A will have two different points on B, leading to two superpontetials indicating a bifurcation behaviour in parameter domain [75]. Similar behaviour is observed for parameter B as well. On the other hand, if for a certain perturbation to the parameters, one reaches the exceptional point then on the opposite path one can move either through the hyperbola one had been originally along or the conjugate hyperbola, making jumps from one superpotential to another possible. As will be explicated in the following section, two superpotentials which characterize the complex Scarf II potential

describe the energy eigenvalues in regions of the $\mathcal{PT}$-unbroken phase separated by the conditions of isospectral deformation and $\mathcal{PT}$-symmetry breaking, where the two energy eigenvalue sets merge. However, the superpotentials do not merge at the isopectral deformation, while they merge for the $\mathcal{PT}$-symmetry breaking as shown in Fig. 2. The hyperbolic nature of the difference between the two ground state energy representations which asymptotically tend to the $\mathcal{PT}$-breaking show the $\mathcal{PT}$ phase transition. SUSY broken regions as shown in Fig. 1 can be considered to be arising due to isospectral deformations which follows independently from the Bernoulli equation. Together Fig. 1 and Fig. 2 depict four parameter domains for energy representation.

5 Broken $\mathcal{PT}-$symmetric phase

For $C^{\mathcal{PT}} \neq 0$, one finds: $A = B - \frac{\alpha}{2}$, which on substituting in Eq. 13, yields

$$W_{\mathcal{PT}}^{\pm} = \left(A \pm iC^{\mathcal{PT}}\right)tanh\,\alpha x + \left(\pm C^{\mathcal{PT}} + i(A + \frac{\alpha}{2})\right)sech\,\alpha x. \tag{29}$$

It is to be noted that both the superpotentials lead to the same $\mathcal{PT}-$symmetric complex potential, corresponding to broken $\mathcal{PT}$-symmetry. Invoking the shape invariance condition, one can obtain the complex energy spectra,

$$E_n^{\pm} = -(A - n\alpha \pm iC^{\mathcal{PT}})^2. \tag{30}$$

The complex conjugate pair of energy eigenvalues are associated with either of the two superpotentials in Eq. 29. The corresponding eigenfunctions are given by,

$$\begin{aligned}
\psi_n^{\pm}(x) &\propto \left(sech\,\alpha x\right)^{\frac{1}{\alpha}(A \pm iC^{\mathcal{PT}})} \exp\Big[-\frac{i}{\alpha}(A + \frac{\alpha}{2} \mp iC^{\mathcal{PT}}) \\
&\quad tan^{-1}(sinh\,\alpha x)\Big] P_n^{\mp\frac{2iC^{\mathcal{PT}}}{\alpha}, -\frac{2A}{\alpha}-1}[i\,sinh\,\alpha x].
\end{aligned} \tag{31}$$

This pair of wavefunctions are related to each other with $\mathcal{PT}$ transformations. Here, $P_n^{\mp\frac{2iC^{\mathcal{PT}}}{\alpha}, -(\frac{2A}{\alpha}+1)}[i\,sinh\,\alpha x]$ is the nth order Jacobi polynomial. The normalizability of ground state wavefunction requires that SUSY remains intact in broken $\mathcal{PT}$ domain. It is also worthwhile to notice that, inspite of being in broken $\mathcal{PT}$-phase, at points $A = n\alpha$, complex eigenmodes have energy eigenvalue, $E_{SS} = C^{\mathcal{PT}^2}$, constituting the zero-width resonances [76] with conditions identical to the one in [66].

6 Conclusion

In conclusion, complex refractive index profile with $\mathcal{PT}$ and SUSY is investigated for understanding of broken and unbroken phases of the two symmetries and their interconnection. The broken and unbroken phases of $\mathcal{PT}$ have been found to exist in mutually exclusive domains.

For $\mathcal{PT}$ unbroken case, the two superpotentials, interconnected by a parametric transformation, lead to a unique potential. The parameter domains are identified where $\mathcal{PT}-$symmetry is preserved but SUSY breaking happens. In these domains, one needs to exploit a non-trivial shape invariance to obtain the corresponding energy spectra. On the other hand, the broken phase of $\mathcal{PT}$ accommodates complex energy spectra with preserving SUSY in the entire parameter range, yielding zero-width resonance states at integral values of A. Moreover, the parametric conditions for isospectral deformation, connecting the two superpotentials describing the same potential in the $\mathcal{PT}$-unbroken phase, is found to be associated with the modified KdV equation of a specific kind. The intersecting lines clearly demarcate the $\mathcal{PT}$-symmetry breaking boundary as well as the isospectral deformation criteria, along which lie points connecting the deformations associated with the modified KdV equation.

Recently $\mathcal{PT}-$symmetric crystals have been experimentally realized with bulk boundary dynamics and topology, in photonic graphene [77]. $\mathcal{PT}-$symmetric phonon lasers have also been proposed theoretically [78] and shown experimentally in optomechanical systems [79], which will enable $\mathcal{PT}$-symmetry phononics akin to the photonic domain. $\mathcal{PT}$-symmetry has been observed in dissipative systems in ultracold atoms [80]. All these systems need careful study both from symmetry prospective as well as for technical applications [81]. $\mathcal{PT}$ symmetry have manifested in kicked top [82], intensity-intensity correlation [83] and other physical systems [84]. The physical phenomena near the exceptional points have been in the forefront area of research, revealing many counter-intuitive effects associated with it. Similarly, dynamical systems with solitonic excitations have been under investigation for the effect of $\mathcal{PT}-$symmetry on this extended objects. We hope to use the understanding gained from this exactly solvable system for throwing light on some of these phenomena in near future.

References

[1] Ye D, Chang K, Ran L, Xin H. 2014 Microwave gain medium with negative refractive index. *Nature Communications* **5**, 5841.

[2] Forcella D, Prada C, Carminati R. 2017 Causality, nonlocality, and negative refraction. *Phys. Rev. Lett.* **118**, 134301. (doi.org/10.1103/PhysRevLett.118.134301)

[3] Park C M, Lee S H. 2019 Zero-reflection acoustic metamaterial with a negative refractive index. *Sci. Rep.* **9** 3372. (doi.org/10.1038/s41598-019-40184-7)

[4] Bender C M, Boettcher S. 1998 Real Spectra in non-Hermitian Hamiltonians having $\mathcal{PT}$ symmetry. *Phys. Rev. Lett.* **80**, 5243. (doi.org/10.1103/PhysRevLett.80.5243)

[5] Bender C M, Brody D C, Jones H F C. 2002 Complex extension of quantum mechanics. *Phys. Rev. Lett.* **89**, 270401. (doi.org/10.1103/PhysRevLett.89.270401)

[6] El-Ganainy R, Makris K G, Christodoulides D N, Musslimani Z H. 2007 Theory of coupled optical PT-symmetric structures. *Opt. Lett. 32*, 2632. (doi.org/10.1364/OL.32.002632)

[7] Guo A, Salamo G J, Duchesne D, Morandotti R, Volatier-Ravat M, Aimez V, Sivilogou G A, Christodoulides D N. 2009 Observation of $\mathcal{PT}$-symmetry breaking in complex optical potentials. *Phys. Rev. Lett. 103*, 093902. (doi.org/10.1103/PhysRevLett.103.093902)

[8] Perego A M, Turitsyn S K, Staliunas K. 2018 Gain through losses in nonlinear optics. *Light Sci. Appl.* **7** 43. (doi.org/10.1038/s41377-018-0042-9)

[9] Parto M, Liu Y G N, Bahari B, Khajavikhan M, Christodoulides D N. 2021 Non-Hermitian and topological photonics: optics at an exceptional point. *Nanophotonics* **10** 403. (doi.org/10.1515/nanoph-2020-0434)

[10] Wilkey A, Suelzer J, Joglekar Y N, Vemuri G. 2019 Parity–Time symmetry in bidirectionally coupled semiconductor lasers. *Photonics* **6**, 122 and references therein. (doi.org/10.3390/photonics6040122)

[11] Zhang F, Feng Y, Chen X, Ge L, Wan W. 2020 Synthetic anti-PT symmetry in a single microcavity. *Phys. Rev. Lett.* **124**, 053901. (doi.org/10.1103/PhysRevLett.124.053901)

[12] Nair J M P, Mukhopadhyay D and Agarwal G S. 2021 Enhanced sensing of weak anharmonicities through coherences in dissipatively coupled anti-PT symmetric systems. *Phys. Rev. Lett.* **126**, 180401. (doi.org/10.1103/PhysRevLett.126.180401)

[13] Farhat M, Yang M, Ye Z, Chen P-Y. 2020 PT-Symmetric absorber-laser enables electromagnetic sensors with unprecedented sensitivity. *ACS Photonics* **7**, 2080. (doi.org/10.1021/acsphotonics.0c00514)

[14] Karthiga S, Chandrasekar V K, Senthilvelan M, Lakshmanan M. 2016 Twofold $\mathcal{PT}$ symmetry in nonlinearly damped dynamical systems and tailoring $\mathcal{PT}$ regions with position-dependent loss-gain profiles. *Phys. Rev. A* **93**, 012102. (doi.org/10.1103/PhysRevA.93.012102);
Govindarajan A, Sarma A K and Lakshmanan M. 2019 Tailoring$\mathcal{PT}$-symmetric soliton switch. *Opt. lett.* **44**, 663. (doi.org/10.1364/OL.44.000663)

[15] Li H, Mekawy A, Krasnok A, Alù A. 2020 Virtual Parity-Time symmetry. *Phys. Rev. Lett.* **124**, 193901. (doi.org/10.1103/PhysRevLett.124.193901)

[16] Öztürk F E, Lappe T, Hellmann G, Schmitt J, Klaers J, Vewinger F, Kroha J, Weitz M. 2021 Observation of a non-Hermitian phase transition in an optical quantum gas. *Science* **372**, 88. (doi.org/10.1126/science.abe9869)

[17] Wess J, Bagger J. 1992 *Supersymmetry and Supergravity* Priceton University Press: Princeton.

[18] Heinrich M, Miri M-A, Stützer S, El-Ganainy R., Nolte S, Szameit A, Christodoulides D N. 2014 Supersymmetric mode converters. *Nat. Commun.* **5**, 3698. (doi.org/10.1038/ncomms4698)

[19] Macho A, Llorente R, García-Meca C. 2018 Supersymmetric transformations in optical fibers. *Phys. Rev. Appl.* **9**, 014024. (doi.org/10.1103/PhysRevApplied.9.014024)

[20] Hokmabadi M P, Nye N S, El-Ganainy R, Christodoulides D N, Khajavikhan M. 2019 Supersymmetric laser arrays. *Science* **363**, 623. (doi.org/10.1126/science.aav5103)

[21] Rüter C E, Makris K G, El-Ganainy R, Christodoulides D N, Segev M, Kip D. 2010 Observation of parity–time symmetry in optics. *Nat. Phys.* **6**, 192. (doi.org/10.1038/nphys1515)

[22] Miri M-A, Heinrich M, El-Ganainy R, Christodoulides D N. 2013 Supersymmetric optical structures *Phys. Rev. Lett.* **110**, 233902. (doi.org/10.1103/PhysRevLett.110.233902)

[23] Principe M, Castaldi G, Consales M, Cusano A, Galdi V. 2015 Supersymmetry-inspired non-Hermitian optical couplers. *Sci. Rep.* **5**, 8568. (doi.org/10.1038/srep08568)

[24] Govindarajan A, Malomed B A, Lakshmanan M. 2019 Nonlinear anti-directional couplers with gain and loss. *Opt. lett.* **44**, 4650. (doi.org/10.1364/OL.44.004650)

[25] Makris K G, El-Ganainy R, Christodoulides D N. 2008 Beam dynamics in $\mathcal{PT}$ symmetric optical lattices *Phys. Rev. Lett.* **100**, 103904. (doi.org/10.1103/PhysRevLett.100.103904)

[26] Kepesidis K V, Milburn T J, Huber J, Makris K G, Rotter S and Rabl P. 2016 $\mathcal{PT}$-symmetry breaking in the steady state of microscopic gain–loss systems. *New J. Phys.* **18**, 95003. (doi.org/ 10.1088/1367-2630/18/9/095003)

[27] Goldzak T, Mailybaev A A, Moiseyev N. 2018 Light stops at exceptional points. *Phys. Rev. Lett.* **120**, 013901. (doi.org/10.1103/PhysRevLett.120.013901)

[28] Dutt R, Khare A, Sukhatme U P. 1988 Supersymmetry, shape invariance, and exactly solvable potentials. *Am. J. Phys.* **56**, 163. (doi.org/10.1119/1.15697)

[29] García-Meca C, Ortiz A M and Sáez R L. 2020 Supersymmetry in the time domain and its applications in optics. *Nat. Commun.* **11**, 813. (doi.org/10.1038/s41467-020-14634-0)

[30] Gendenshtein L E. 1983 Derivation of exact spectra of the Schr0dinger equation by means of supersymmet *JETP Lett.* **38**, 356.

[31] Bougie J, Gangopadhyaya A, Jeffry V, Mallow J V. 2010 Generation of a complete set of additive shape-invariant potentials from an Euler equation. *Phys. Rev. Lett.* **105**, 210402. (doi.org/10.1103/PhysRevLett.105.210402)

[32] Cooper F, Khare A, Sukhatme U P. 2001 *Supersymmetry in Quantum Mechanics*; World Scientific: Singapore and references therein.

[33] Dutta S K, Gupta D, Saha S K. 2018 Resonance state wave functions of ^{15}Be using supersymmetric quantum mechanics *Phys. Lett. B* **776**, 464. (doi.org/10.1016/j.physletb.2017.12.008)

[34] Musslimani Z H, El-Ganainy R, Makris K G, Christodoulides D N. 2008 Optical solitons in $\mathcal{PT}$ periodic potentials. *Phys. Rev. Lett.* **100**, 030402. (doi.org/10.1103/PhysRevLett.100.030402)

[35] Alexeeva N V, Barashenkov I V, Sukhorukov A A, Kivshar Y S. 2012 Optical solitons in $\mathcal{PT}$-symmetric nonlinear couplers with gain and loss. *Phys. Rev. A* **85**, 063837. (doi.org/10.1103/PhysRevA.85.063837)

[36] Kumar C N, Gupta R, Goyal A, Loomba S, Raju T S, Panigrahi P K. 2012 Controlled giant rogue waves in nonlinear fiber optics. *Phys. Rev. A* **86**, 025802. (doi.org/10.1103/PhysRevA.86.025802)

[37] Abhinav K, Panigrahi P K. 2010 Supersymmetry, PT-symmetry and spectral bifurcation. *Ann. Phys.* **325**, 1198 and references therein. (doi.org/10.1016/j.aop.2010.04.003);
Bagchi B, Quesne C. 2011 Comment on 'Supersymmetry, PT-symmetry and spectral bifurcation'. *Ann. Phys.* **326**, 534. (doi.org/10.1016/j.aop.2010.10.007);
Abhinav K, Panigrahi P K. 2011 Comment on 'Supersymmetry, PT-symmetry and spectral bifurcation'. *Ann. Phys. 326*, 538. (doi.org/10.1016/j.aop.2010.10.007)

[38] Miri M-A, Alú A 2019 *Science* **2019** *363* 957.

[39] Regensburger A, Bersch C, Miri M-A, Onishchukov G, Christodoulides D N, Peschel U. 2012 Parity-time synthetic photonic lattices. *Nature* **488**, 168.(doi.org/10.1038/nature11298)

[40] Klaiman S, Günther U, Moiseyev N. 2008 Visualization of branch points in $\mathcal{PT}$-symmetric waveguides *Phys. Rev. Lett.* **101**, 080402. (doi.org/10.1103/PhysRevLett.101.080402)

[41] Čtyroký J, Kuzmiak V, Eyderman S. 2010 Waveguide structures with antisymmetric gain/loss profile. *Opt. Expr.* **18**, 21585. (doi.org/10.1364/OE.18.021585)

[42] Lv B, Fu J, Wu B, Li R, Zeng Q, Yin X, Wu Q, Gao L, Chen W, Wang Z, Liang Z, Li A, Ma R. 2017 Unidirectional invisibility induced by parity-time symmetric circuit. *Sci. Rep.* **7**, 40575. (doi.org/10.1038/srep40575)

[43] Miri M-A, Regensburger A, Peschel U, Christodoulides D N. 2012 Optical mesh lattices with $\mathcal{PT}$ symmetry. *Phys. Rev. A* **86**, 023807. (doi.org/10.1103/PhysRevA.86.023807)

[44] Zhang Z, Zhang Y, Sheng J, Yang L, Miri M-A, Christodoulides D N, He B, Zhang Y, Xiao M. 2016 Observation of Parity-Time symmetry in optically induced atomic lattices. *Phys. Rev. Lett.* **117**, 123601. (doi.org/10.1103/PhysRevLett.117.123601)

[45] Kuo P C, Lambert N, Miranowicz A, Chen H B, Chen G Y, Chen Y N, Nori F. 2020 Collectively induced exceptional points of quantum emitters coupled to nanoparticle surface plasmons. *Phys. Rev. A* **101**, 013814. (doi.org/10.1103/PhysRevA.101.013814)

[46] Longhi S. 2018 Quantum interference and exceptional points. *Opt. Lett.* **43**, 2929. (doi.org/10.1364/OL.43.005371)

[47] Ramezan H. 2017 Non-Hermiticity-induced flat band. *Phys. Rev. A* **96**, 011802(R). (doi.org/10.1103/PhysRevA.96.011802)

[48] Fleury R, Sounas D L, Alú A. 2014 Negative refraction and planar focusing based on Parity-Time symmetric metasurfaces. *Phys. Rev. Lett.* **113**, 023903. (doi.org/10.1103/PhysRevLett.113.023903)

[49] Longhi S. 2009 Bloch oscillations in complex crystals with $\mathcal{PT}$ symmetry. *Phys. Rev. Lett.* **103**, 123601. (doi.org/10.1103/PhysRevLett.103.123601)

[50] Longstaff B, Graefe E-M. 2019 Nonadiabatic transitions through exceptional points in the band structure of a $\mathcal{PT}$-symmetric lattice. *Phys. Rev. A* **100**, 052119. (doi.org/10.1103/PhysRevA.100.052119)

[51] Bender C M. 2016 PT symmetry in quantum physics: From a mathematical curiosity to optical experiments. *Europhysics News.* **47**, 1720. (doi.org/10.1051/epn/2016201)

[52] Gupta S D, Agarwal G S. 2007 A new approach for broad-band omnidirectional antireflection coatings. *Opt. Expr.* **15**, 9614. (doi.org/10.1364/OE.15.009614)

[53] Thekkekara L V, Gopal Achanta V, Gupta S D. 2014 Optical reflectionless potentials for broadband, omnidirectional antireflection. *Opt. Expr.* **22**, 17382. (doi.org/10.1364/OE.22.017382)

[54] Contreras-Astorga A, Jakubský V. 2019 Photonic systems with two-dimensional landscapes of complex refractive index via time-dependent supersymmetry. *Phys. Rev. A* **99**, 053812. (doi.org/10.1103/PhysRevA.99.053812)

[55] Chen Y, Yan Z, Mihalache D, Malomed B A. 2017 Families of stable solitons and excitations in the PT-symmetric nonlinear Schrödinger equations with position-dependent effective masses. *Sci. Rep.* **7**, 1257. (doi.org/10.1038/s41598-017-01401-3)

[56] Miri M-A, Heinrich M, Christodoulides D N. 2013 Supersymmetry-generated complex optical potentials with real spectra. *Phys. Rev. A* **87**, 043819. (doi.org/10.1103/PhysRevA.87.043819)

[57] Khare A, Sukhatme U P. 1988 Scattering amplitudes for supersymmetric shape-invariant potentials by operator methods. *J. Phys. A: Math. Gen.* **21**, L501. (doi.org/10.1088/0305-4470/21/9/005)

[58] Lévai G, Znojil M. 2002 The interplay of supersymmetry and PT symmetry in quantum mechanics: a case study for the Scarf II potential. *J. Phys. A: Math. Gen.* **35**, 8793. (doi.org/10.1088/0305-4470/35/41/311)

[59] Lévai G. 1994 Solvable potentials associated with su(1,1) algebras: a systematic study. *J. Phys. A: Math. Gen.* **27**, 3809. (doi.org/10.1088/0305-4470/27/11/031)

[60] Lévai G, Cannata F, Ventura A. 2001 Algebraic and scattering aspects of a $\mathcal{PT}$-symmetric solvable potential *J. Phys. A: Math. Gen.* **34**, 839. (doi.org/10.1088/0305-4470/34/4/310)

[61] Gangopadhyaya A, Panigrahi P K, Sukhatme U P. 1994 Inter-relations of solvable potentials. *Helv. Phys. Acta* **67**, 363.

[62] Pöschl G, Teller E. 1933 Bemerkungen zur Quantenmechanik des anharmonischen Oszillators *Z. Phys.* **83**, 143. (doi.org/10.1007/BF01331132)

[63] Alhassid Y, Gürsey F, Iachello F. 1983 Group theory approach to scattering. *Ann. Phys.* **50**, 873. (doi.org/10.1016/0003-4916(83)90244-0)

[64] Díaz J I, Negro J, Nieto L M, Rosas-Ortiz O. 1999 The supersymmetric modified Pöschl-Teller and delta well potentials. *J. Phys. A: Math. Gen.* **32**, 8447. (doi.org/10.1088/0305-4470/32/48/308)

[65] Abhinav K, Jayannavar A, Panigrahi P K. 2013 Conserved correlation in $\mathcal{PT}$-symmetric systems: Scattering and bound states *Ann. Phys.* **331**, 110. (doi.org/10.1016/j.aop.2013.01.002)

[66] Ahmed Z. 2001 Real and complex discrete eigenvalues in an exactly solvable one-dimensional complex $\mathcal{PT}$-invariant potential *Phys. Lett. A* **282**, 343. (doi.org/10.1016/S0375-9601(01)00218-3)

[67] Bagchi B, Quesne C 2002 *Phys. Lett. A* **300**, 18. Non-Hermitian Hamiltonians with real and complex eigenvalues in a Lie-algebraic framework. (10.1016/S0375-9601(02)00689-8);
Sree Ranjini S, Kapoor A K and Panigrahi P K. 2005 Quantum Hamiltonian–Jacobi analysis of $\mathcal{PT}$ symmetric Hamiltonians. *Int. J. Mod. Phys. A* **20**, 4067. (doi.org/10.1142/S0217751X05022810)

[68] Yadav R K, Khare A, Bagchi B, Kumari N, Mandal B P. 2016 Parametric symmetries in exactly solvable real and PT symmetric complex potentials. *J. Math. Phys.* **57**, 062106. (doi.org/10.1063/1.4954330)

[69] Bagchi B, Quesne C. 2000 sl(2, C) as a complex Lie algebra and the associated non-Hermitian Hamiltonians with real eigenvalues. *Phys. Lett. A* **273**, 285. (doi.org/10.1016/S0375-9601(00)00512-0)

[70] Gangopadhyaya A, Mallow J V, Sukhatme U P. 2001 Broken Supersymmetric shape invariant systems and their potential algebras. *Phys. Lett. A* **283**, 279. (doi.org/10.1016/S0375-9601(01)00266-3)

[71] Rasinariu C, Mallow J V, Gangapadhyaya A. 2007 Exactly solvable problems of quantum mechanics and their spectrum generating algebras: A review. *CEJP* **5**, 111. (doi.org/10.2478/s11534-007-0001-1)

[72] Flugge S. 1999 *Practical Quantum Mechanics*; Springer-Verlag: Berlin, Heidelberg and references therein.

[73] Kevrekidis P G, Khare A, Saxena A. 2003 Breather lattice and its stabilization for the modified Korteweg–de Vries equation. *Phys. Rev. E* **68**, 047701. (doi.org/10.1103/PhysRevE.68.047701)

[74] Modak S, Singh A P, Panigrahi P K. 2016 Complex solitary waves and soliton trains in KdV and mKdV equations. *Eur. Phys. J. B* **89**, 149. ((doi.org/10.1140/epjb/e2016-70130-7))

[75] Sakhi S, Panigrahi P K. 2019 Bifurcation of fixed points in a O(N)-symmetric $(2 + 1)-$dimensional gauged Φ^6 theory with a Chern-Simons term *Phys. Rev. D* **99**, 036017. (doi.org/10.1103/PhysRevD.99.036017)

[76] Mostafazadeh A. 2011 Optical spectral singularities as threshold resonances. *Phys. Rev. A* **83**, 045801. (doi.org/10.1103/PhysRevA.83.045801)

[77] Kremer M, Biesenthal T, Heinrich M, Thomale R, Szameit A 2018 *arXiv:1809.00041*. (arxiv.org/abs/1809.00041)

[78] Jing H, Özdemir S K, Lü X, Zhang J, Yang L, Nori F. 2014 $\mathcal{PT}$-symmetric phonon laser *Phys. Rev. Lett.* **113**, 053604. (doi.org/10.1103/PhysRevLett.113.053604)

[79] Xiao X, Liao Q, Zhou N, Nie W, Liu Y. 2020 Tunable optical second-order sideband effects in a parity-time symmetric optomechanical system. *Sci. China Phys. Mech. Astron.* **63**, 114211. (doi.org/10.1007/s11433-020-1559-4)

[80] Li J, Harter A K, Liu J, Melo L de, Joglekar Y N, Luo L. 2019 Observation of parity-time symmetry breaking transitions in a dissipative Floquet system of ultracold atoms. *Nature Communications* **10**, 855. (doi.org/10.1038/s41467-019-08596-1)

[81] Joglekar Y N, Scott D, Babbey M, Saxena A. 2010 Robust and fragile $\mathcal{PT}$-symmetric phases in a tight-binding chain. *Phys. Rev. A* **82**, 030103(R). (doi.org/10.1103/PhysRevA.82.030103)

[82] Mudute-Ndumbe S, Graefe E-M. 2020 A non-Hermitian PT-symmetric kicked top. *New Journal of Physics* **22**, 103011. (doi.org/10.1088/1367-2630/abb27a)

[83] Graefe E-M. 2019 PT symmetry dips into two-photon interference. *Nature Photonics* **13**, 822. (doi.org/10.1038/s41566-019-0551-y)

[84] Gunderson J, Muldoon J, Murch K W, Joglekar Y N. 2021 Floquet exceptional contours in Lindblad dynamics with time-periodic drive and dissipation. *Phys. Rev. A* **103**, 023718. (doi.org/10.1103/PhysRevA.103.023718)